# ON THE INFLUENCE OF OVERLAP TOPOLOGY ON TENSILE STRENGTH OF COMPOSITE BONDED JOINTS: A MULTI-STACKING DESIGN

J. Kupski[*,1], S. Teixeira de Freitas[1], D. Zarouchas[1], R. Benedictus[1]

[1]Structural Integrity & Composite Group, Faculty Aerospace Engineering, Delft University of Technology, Kluyverweg 1, 2629HS, NL
Email: j.a.kupski@tudelft.nl

**Keywords:** Composite joints, adhesive bonding, finger joints, joint topology

**Abstract**
The goal of this study is to investigate new designs of composite bonded joints in order to improve their strength under tensile loading. Multiple stacked overlaps are compared with single overlap designs. The concept of multiple stacking is well known as ply-interleaving technique for co-curing dissimilar materials. For a secondary bonding process, a similar concept is used in tongue-and-groove joints. However, it is so far limited to one stacking level due to the complexity of the design. By means of thin unidirectional layers, the tongue-and-groove design is expanded further to two stacking sequences and applied to secondary bonding of CFRP adherends.
Single lap joints of 12.7 and 25.4 mm overlap length were compared to finger joints with 1 and 2 overlaps of 12.7 mm overlap length, stacked through the thickness. Specimens were tested according to ASTM D-5868-01. The initial and final failure load were recorded.
The study shows that for the same overlap length in a multi-stacked configuration, there is a potential for higher average lap strength, in comparison with an increase in overlap length of a single overlap. This effect might be mainly due to the reduction of secondary bending moment and by load distribution over multiple interfaces.

## 1. Introduction

Since the launch of Boeing's 787 Dreamliner, airplane fuselage structures made out of Carbon Fibre Reinforced Plastic (CFRP) were fully introduced in civil aviation. Adhesive bonding is one of the most suitable joining technology in terms of weight and performace for current CFRP fuselage structures. However, traditional joint topologies such as single overlap joints (SLJ) induce high peel stresses into the composite adherends thickness direction, resulting in sudden failure and low joint strength when compared to metal adherends [1-2]. As a result, current safety-critical bonded joints are always used in combination with redundant fastners. This practice is jeopardizing the weight-efficieny of full-scale composite structures, where joints are essential.

Compared to the traditional SLJ-design, mainly chosen due to the easiness of manufacture [3], finger joints (FJ) could be a promising alternative to increase joint strength due to a more gradual load transfer to the composite adherends as they lead to lower peel stresses [1]. FJs, also referred as tongue-and-groove joints, are a well-known design in the wood industry [4], where slots are created by profiling the bonding surface with a rotational milling tool. In Fiber Reinforced Polymers (FRP), FJ-topologies have been mostly studied for thick laminates (>10 mm thickness), such as Glass Fibre

Reinforced Plastic (GFRP) and sandwich structures, to connect, for example, components of wind turbine blades [7]. Another studied application of the FJ topologies is the interleaving technique of single plies, when building up FRP laminates. This method is mainly used to laminate heterogeneous adherends, such as CFRP/GFRP, which are then co-cured in one single cycle [8].
However, FJs have not been studied for secondary bonding of CFRP structures, most probably because the thickness of the CFRP laminates is often very thin (<5 mm, e.g. for an Airbus A350-900 XWB fuselage panel [5]). Moreover, the CFRP finger slots can hardly be milled, as common milling tools still suffer enormous deterioration from processing CFRP products [6]. These manufacturing issues have so far been hindering further investigation of FJ topologies for CFRP aircraft fuselage panels.
In order to explore the advantages of FJ-designs as an alternative to SLJ, this paper proposes to use a multi-stacking joint design for secondary bonding of thin CFRP panels. The ply-interleaving technique is applied onto a secondary adhesive bonding process on monolithic CFRP adherends with aerospace-grade elastic properties that correspond to the design of a typical fuselage panel.
The aim of the study is to investigate whether an increase of overlap length, stacked through the thickness of the laminate, provides increase in tensile joint strength when compare to an increase of overlap length along one bond line of the SLJ-design.

## 2. Experimental Methods

### 2.1 Materials

The materials used for this study are unidirectional (UD) prepreg tapes from carbon fibres and epoxy resin for the composite adherends and an epoxy film adhesive for the bondline.
The Prepreg tape is Hexply® 6376C-HTS(12K)-5-35% (Hexcel Composites in Duxford, UK), containing high tenacity Tenax®-E HTS45 standard modulus fibres (Toho Tenax Europe GmbH) and the Hexply® 6376 thermoplastic-toughened epoxy matrix system. The adhesive is Scotch-Weld™ AF 163-2K in 293 g/m$^2$ areal weight, including a knit supporting carrier, from 3M Netherlands B.V.

### 2.2 Specimen

Two types of joint topologies were tested: SLJ-designs with two overlap lengths (OL) of 12.7 and 25.4 mm, and FJ-designs with one and two stacked overlaps at a constant overlap length of 12.7 mm, see Figure 1. The composite adherends of these 4 design configurations were manufactured in two cross-ply layups $[0/90]_{4s}$ and $[90/0]_{4s}$. Specimens were built according to ASTM standard D 5868-01 [9], with a constant width of 25.4 mm. The composite adherends consist of 16 UD-layers of 0.125 mm single ply thickness. Table 1 summarizes the eight design configurations, investigated throughout this study.


**Figure 1:** SLJ-designs and. FJ-designs tested.

**Table 1:** Design configurations tested.

| Design | Adherend's layup | overlap length [mm] |
|---|---|---|
| SLJ-1-0/90 | $[0/90]_{4s}$ | 12.7 |
| SLJ-2-0/90 | $[0/90]_{4s}$ | 25.4 |
| SLJ-1-90/0 | $[90/0]_{4s}$ | 12.7 |
| SLJ-2-90/0 | $[90/0]_{4s}$ | 25.4 |
| FJ-1-0/90 | $[0/90]_{4s}$ | 12.7 |
| FJ-2-0/90 | $[0/90]_{4s}$ | 12.7 |
| FJ-1-90/0 | $[90/0]_{4s}$ | 12.7 |
| FJ-2-90/0 | $[90/0]_{4s}$ | 12.7 |

The adherends were laminated in a Prepreg hand layup process, with 15 min of de-bulking at an under pressure lower than 100 mbar between every second layer. The laminates were packed between a base of 12 mm thickness and a caul plate of 2 mm thickness from aluminium. Curing took place in the autoclave at 177 °C and 7 bar gauge pressure for 120 min time.

The adhesive bonding process was performed by laying the uncured film adhesive onto the cured adherends and arranging a vacuum setup around them. Prior to bonding, a surface treatment was applied to the CFRP surface which consisted of the following procedure: (1) degreasing the surface with Acetone, (2) manual grinding with 3M's Scotch Bride™, (3) cleaning with Acetone, and (4) 7 min UV/ozone treatment. Previous studies show that this surface treatment results in good wettability of the CFRP surfaces [10].
The bonding curing process was performed in the autoclave at 2 bar gauge pressure and 120 °C curing temperature for 90 min dwell time.

Adherends of the SLJ-designs had a thickness of 2.0 mm (+/- 0.1 mm) of the CFRP laminate and 0.15 mm (+/- 0.03 mm) of the bondline. In the FJ-specimens, the thickness of the laminate at the OL region was 1.7 mm (+/- 0.1 mm) at the joint region, while the bondline thickness was again 0.15 mm (+/-0.03 mm).

### 2.6 Quasi-static tensile tests

Five specimens per design configuration were tested under to quasi-static tensile loading. The tests were performed under displacement control with a constant displacement rate of 1.3 mm/min. They were performed on a Zwick-Roell AllroundLine Z250 SW testing machine with a load cell of 250 kN. Figure 3 shows the test set up. Specimens were clamped at the ends by two clamps at 250 bar hydraulic pressure. The initial distance of the clamps was set to 200 mm and with a misalignment of 2 mm to counterbalance the overlap offset for the SLJ-configurations, whereas there was no offset needed for the FJ-configurations. Beyond recording the load and displacement from the testing machine, an Acoustic Emission (AE) system by Vallen Systeme GmbH was employed, consisting of two VS900-M sensors, to monitor the acoustic emission activity during the tests. The AE system was connected to the load cell of the test frame in order to synchronize the AE activity with the load measurements. AE-sensors were attached onto the same side of the specimen at +/- 30 mm from the overlap centre and connected to the AEP4H 34dB amplifier,

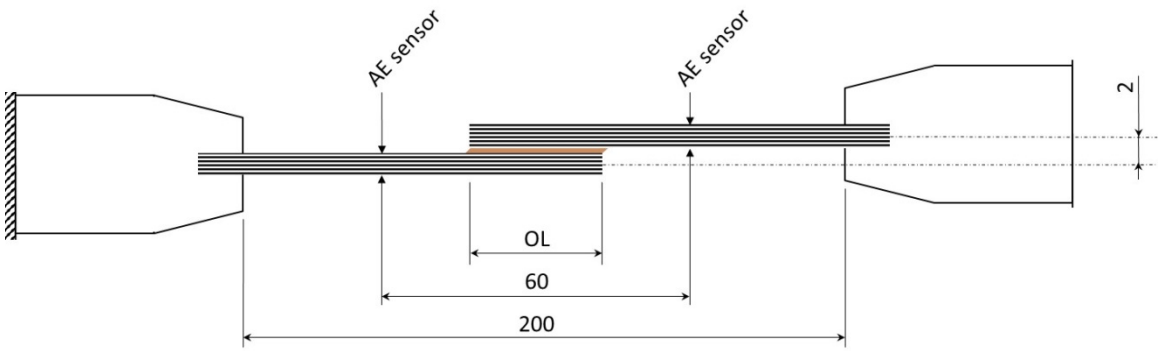


**Figure 3**: Test setup, illustrated for the SLJ-design including clamping offset (dimensions in mm)

## 3 Results

### 3.1 Failure loads

The average lap shear strength $\sigma_{LSS}$ of each specimen was derived from the maximum load recorded during test, divided by the initial overlap area of each specimen. For the FJ-designs, a constant OL of 12.7 mm was considered, regardless of the number of fingers. The values for average shear stress at damage initiation $\sigma_{init}$ were derived by correlating the sudden increase of cummulative AE hits with the corresponding load. An example of how the initial failure load was determined is presented in Figure 4. The dashed line indicates the load [N] over time [s] and the marked lines represent the cumulative number of acoustic hits over time [s] for one specimen of configuration SLJ-2-0/90 with 25.4 mm OL. A sudden increase of inclination of cummulative hits for both AE-sensors at 12 s indicates the event of a damage initiation at 2050 N for this specimen. The same procedure was followed for all tested samples.

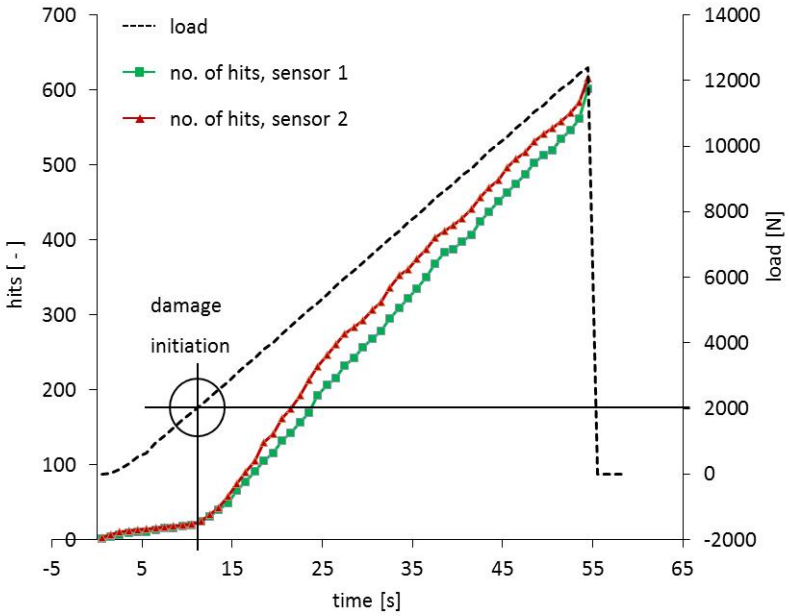


**Figure 4:** Deriving AE-results for a SLJ specimen of layup $[0/90]_{4s}$ and 25.4 mm OL

Table 2 shows the average lap shear strength at final failure and the average shear stress at damage initiation for all specimens tested. These results are also shown in plot graphs in Figure 5. SLJ-designs

show no large deviation between different OL, although there is a tendency of slight decrease in $\sigma_{LSS}$ towards larger OL noticeable. For the FJ-design however, $\sigma_{LSS}$ doubles from 1 to 2 fingers. This trend is observed for both composite adherend's layups, whereas $[90/0]_{4s}$ promotes slightly higher maximum strength than [0/90]. There is a similar trend visible for strength at initial failure ($\sigma_{init}$), although at much lower values.

**Table 2:** Average lap shear stress at at initial failure $\sigma_{init}$ and final failure $\sigma_{LSS}$ ( ±standard deviation)

| design | $\sigma_{init}$ [MPa] | $\sigma_{LSS}$ [MPa] |
|---|---|---|
| SLJ-1-0/90 | 5.5 (± 0.6) | 32.9 (± 1.4) |
| SLJ-2-0/90 | 2.7 (± 0.4) | 30.5 (± 1.5) |
| SLJ-1-90/0 | 5.6 (± 0.4) | 23.7 (± 2.4) |
| SLJ-2-90/0 | 3.0 (± 0.5) | 19.1 (± 0.8) |
| FJ-1-0/90 | 4.2 (± 0.2) | 26.3 (± 2.1) |
| FJ-2-0/90 | 7.9 (± 0.7) | 49.4 (± 6.9) |
| FJ-1-90/0 | 2.2 (± 0.7) | 24.6 (± 1.4) |
| FJ-2-90/0 | 11.1 (± 1.0) | 53.6 (± 2.0) |

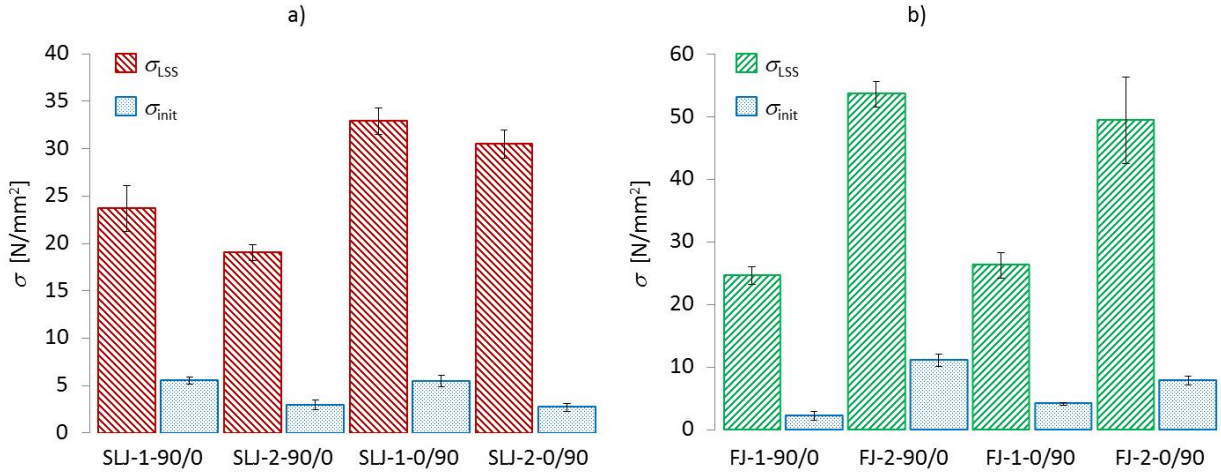


**Figure 5:** Average lap shear strength vs. strength at initial failure, for SLJ- (a) and FJ-designs (b) in $[90/0]_{4s}$ and $[0/90]_{4s}$

### 3.2 Fracture surfaces

In Figures 6 and 7, the typical fracture surfaces for each specimen configuration are illustrated. As can be seend in Figure 6, the SLJ-1-0/90 design resulted in a mixed fracture surface with a crack partly propagating through the adhesive and partly along the 1st layer (0°) adjacent to the bond line. For the SLJ-2-0/90 design cohesive failure inside the adhesive is mostly observed. The design configurations with 90° adjacent to the bondline (SLJ-1-90/0, SLJ-2-90/0) show interlaminar failure inside the composite, between 1st (90°) and 2nd layer (0°) and no trace of cracks propagating throught the adhesive bondline. In the case of SLJ-2-90/0 the crack split up at ca. 40% OL and jumped perpendicular to the bond line thickness until reaching between 1st (90°) and 2nd (0°) layer of the opposite adherend again.

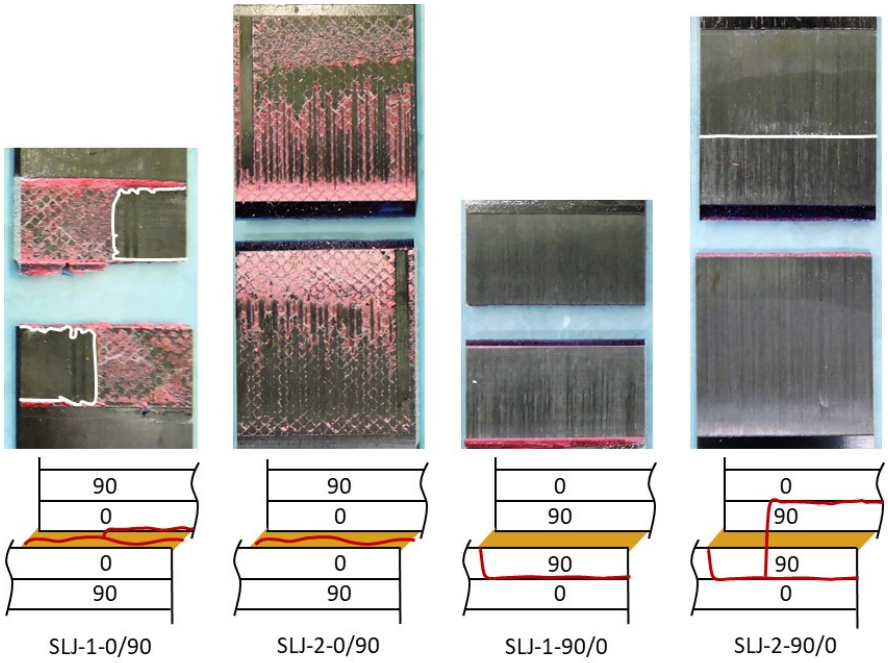


**Figure 6:** Exposed final fracture surfaces of SLJ-designs

In Figure 7, the fracture surfaces of the FJ are shown. All FJ-designs failed inside the composite. For the FJ-1-0/90 design, failure tended to start at the surface of the adhesive resin pocket, migrating inside the adherend between 1st (0°) and the 2nd (90°) layer adjacent to the bond line. For the 2-finger design FJ-2-0/90 of the same layup, the same mechanism tends to occur, although crack pathes are observed symmetrically on both embracing fingers as a mix of interlaminar failure between 1st (0°) and the 2nd (90°) outside layer and intralaminar failure inside the most outside (0°) layer. The design configurations with 90° adjacent to the bondline (FJ-1-90/0, FJ-2-90/0) show a similar failure pattern to the FJ-1-0/90 design, with interlaminar failure inside the composite, between 1st (90°) and 2nd layer (0°) away from the bond line.

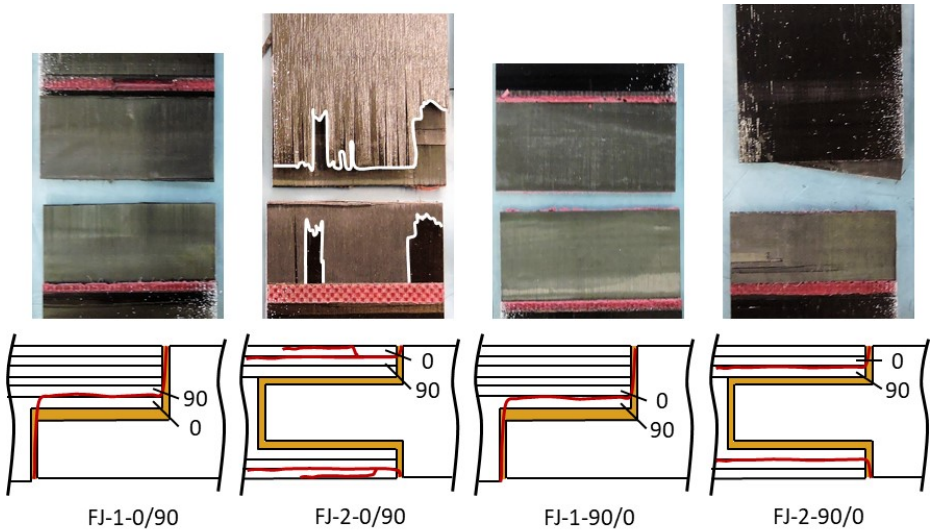


**Figure 7:** Exposed final fracture surfaces of FJ-designs

## 4 Discussion

From the topologies tested, the 2F-design provides the highest joint strength, both until reaching initial damage and until ultimate failure in comparison with the remaining configurations. This effect may appear due to the integrated finger design, where adherends are aligned flatwise. Without joint excentricity, there is no detrimental moment of secondary bending caused. Furthermore, the load transfer through several overlaps might allow for a more consistend stress distribution than for the 1F-design.
However, those high values for average lap shear strength are based on the same OL of 12.7 mm for all FJ-designs. Taking into account the overall adhesive length as 2x 12.7 mm for the 2-finger design against 1x 12.7 mm for the 1-finger design, the absolute shear stress at failure load would show only 6.5 % decrease from FJ-1-0/90 to FJ-2-0/90 and 8.2 % increase from FJ-1-90/0 to FJ-2-90/0.
Comparing SLJ-design and FJ-design and taking again into account the overall adhesive length, the SLJ-design with 90° adjacent to the bond line has a similar absolute shear stress at failure load as the FJ-designs, while the SLJ-0/90 design reaches between 30.5 MPa for SLJ-2-0/90 and 32.9 MPa for SLJ-1-0/90. This result correlates with the observed fracture surfaces in the sense, that all topologies with composite failure result in lower average shear stress at failure between 19.1 MPa (for SLJ-2-90/0) and 26.3 MPa (for FJ-1-0/90), while those topologies with cohesive failure inside the bond line exhibit higher average shear stress at failure load.
A cross-ply stacking sequence of $[90/0]_{4s}$ was chosen to trigger the crack inside the composite adherends, whereas the opposite layup $[0/90]_{4s}$ with 0° adjacent to the bond line would focus the damage more towards the adhesive [14]. Observing this test campaign, all configurations with layup $[90/0]_{4s}$, exhibit indeed the failure inside the composite. In contrast, $[0/90]_{4s}$ FJ-designs failed inside the composite, while SLJ-designs of the same layup, failed inside the adhesive.
Figure 8 reveals how far the crack travelled through the composite adherends of the FJ-2-90/0 design, which correlates with the highest average lap shear strength throughout this test campain.

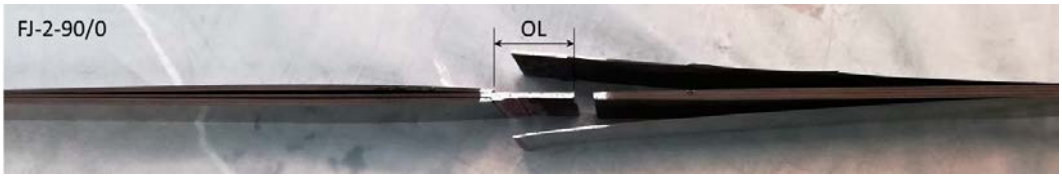


**Figure 8:** FJ-design with 2 fingers and layup $[90/0]_{4s}$ after final failure

## 5 Conclusions

The aim of this study was to understand the effect of a multi-stacked overlap design on the tensile strength of composite bonded joints under quasi-static loading. Based on the results presented, the following conclusions can be drawn:

- The FJ-design shows a potential to increase the average lap shear strength, compared to the SLJ-design. The average lap shear strength could be doubled by replacing a SLJ-design of 25.4 mm OL by a 2 finger design of 12.7 mm OL
- A certain composite adherend layup can stear the crack path. With a stacking sequence of $[90/0]_{4s}$, a crack can be triggered inside the composite. For a layup of $[0/90]_{4s}$, the crack propagation will most likely propagate cohesively along the bond line for SLJ-designs but inside the composite for FJ-designs.
- Aiming for highest average lap shear strength, the FJ-2-90/0 design scored best by provoking the crack to travel far through the composite adherend. However, if the total bondline length is considered instead of the OL, the highest average shear stress at failure was achieved by the SLJ-2-0/90 design with cohesive failure inside the adhesive.

## References

[1] R. D. Adams: *Strength Predictions for Lap Joints, Especially with Composite Adherends. A Review*. J. Adhesion vol. 30, pp. 219-242, 1989

[2] S. Teixeira de Freitas, J. Sinke: *Failure analysis of adhesively-bonded skin-to-stiffener joints: Metal–metal vs. composite–metal*. Eng. Failure Analysis, vol. 56, pp. 2-13, 2015

[3] A.D. Crocombe, I.A. Ashcroft: *Modelling of Adhesively Bonded Joints*. Springer, 2008, Chapter 1: *Simple Lap Joint Geometry*, ISBN: 978-3-540-79055-6

[4] *SPS 1: Special Products Standard for Fingerjoined Structural Lumber*. National Lumber Grades Authority, Vancouver, 2017

[5] I. Sen: *Design of A350 XWB Aircraft fuselage design study: Parametric modelling, structural analysis, material evaluation and optimization for aircraft fuselage*. Master thesis at Delft University of Technology, Faculty of Aerospace Engineering, 2010

[6] E. Uhlmann, F. Sammler, S. Richarz, F. Heitmueller, M. Bilz: *Machining of Carbon Fibre Reinforced Plastics*. Procedia CIRP, vol. 24, pp. 19-24, 2014

[7] G.J.Dvorak, J.Zhang, O.Canyurt: *Adhesive tongue-and-groove joints for thick composite laminates*. Comp. Science and Tech., vol. 61, pp 1123–1142, 2001

[8] J. Ahamed, M. Joosten, P. Callus, S. John, C.H. Wang: *Ply-interleaving technique for joining hybrid carbon/glass fibre composite materials*. Comp.: Part A, vol. 84, pp. 134-146, 2016

[9] ASTM D5868 - 01: *Standard Test Method for Lap Shear Adhesion for Fiber Reinforced Plastic (FRP) Bonding*, 2014

[10] S. Teixeira de Freitas, D. Zarouchas, J.A. Poulis: *The use of acoustic emission and composite peel tests to detect weak adhesion in composite structures*. J. Adhesion, DOI: 10.1080/00218464.2017.1396975, 2018

[11] Material datasheet: *A75-T-2-0123-1-1*. Airbus Material-Handbook Structure, 2014

[12] Material datasheet*: Scotch-Weld™ Structural Adhesive Film AF 163-2AF163-2k*. 3M, Multimedia database, 2009

[13] *Ultraviolet-Ozone Surface treatment*. Three Bond Technical News, vol. 17, 1987

[14] W. J. Renton, J. R. Vinson: *The efficient design of adhesive bonded joints*. J. Adhesion, vol. 7, pp. 175-193, 1975